

## Decay of the $0_2^+$ state in $^{80}\text{Kr}$

A. Giannatiempo

*Dipartimento di Fisica, Università di Firenze, Firenze, Italy  
and Istituto Nazionale di Fisica Nucleare, sezione di Firenze, Firenze, Italy*

A. Nannini

*Istituto Nazionale di Fisica Nucleare, sezione di Firenze, Firenze, Italy*

A. Perego and P. Sona

*Dipartimento di Fisica, Università di Firenze, Firenze, Italy  
and Istituto Nazionale di Fisica Nucleare, sezione di Firenze, Firenze, Italy*

M. J. G. Borge

*Instituto "Estructura de la Materia," Consejo Superior de Investigaciones Científica, Madrid, Spain*

K. Riisager

*Institute of Physics and Astronomy, Aarhus University, Aarhus, Denmark*

O. Tengblad and ISOLDE Collaboration

*CERN, CH-1211 Geneva 23, Switzerland*

(Received 8 September 1992)

The electric monopole strength  $\rho^2$  for the  $0_2^+ \rightarrow 0_1^+$  transition and the  $B(E2)$  value for the  $0_2^+ \rightarrow 2_1^+$  transition were deduced from internal electron conversion and  $\gamma$ -ray spectroscopy and from the measurement of the lifetime of the  $0_2^+$  state, performed by means of the Doppler shift attenuation method in gases. In addition, an upper limit was deduced for the  $E0$  component of the  $2_2^+ \rightarrow 2_1^+$  transition. The available spectroscopic data on low-lying positive parity levels in  $^{78,80,82}\text{Kr}$  are compared to the predictions of the interacting boson model (IBM-2).

PACS number(s): 23.20.Nx, 21.60.Ev, 27.50.+e

### I. INTRODUCTION

The nature of the low-lying  $0^+$  excited states in even even nuclei of the  $A \approx 70-80$  mass region is still an open question (see, for instance Ref. [1] and references therein). Detailed theoretical investigations have mainly been performed in the framework of the interacting boson model (IBM) in its IBM-1 and IBM-2 versions (the latter one distinguishes between neutron and proton bosons). For even krypton isotopes a systematic investigation was performed some time ago by Kaup and Gelberg [2]. By applying the IBM-2 model they satisfactorily reproduced the excitation pattern of the low-lying levels with the exception of the  $0_2^+$  states which were interpreted as "intruder" states lying outside the model space used. Several authors [3-7] starting from the same set of Hamiltonian parameters extended the calculations to include  $E2$  transition rates and obtained a reasonable agreement with experiment.

On the other hand, by applying the IBM-1 model, Erokhina *et al.* [8] were able to reproduce the excitation pattern of the low-lying levels including the  $0_2^+$  states. Moreover, they found a quite reasonable agreement between predicted and experimental values of several  $B(E2)$  transition probabilities in  $^{76,78,80}\text{Kr}$ . However, the lack of experimental data on the transition strengths from the  $0^+$  states in even krypton isotopes did not allow

for a more definite conclusion. Actually, the only experimental study so far reported in the literature concerns the decay of the  $0_2^+$  and  $0_3^+$  states in  $^{82}\text{Kr}$  [9].

As part of an experimental program aimed at a systematic investigation of the  $E0$  and  $E2$  decay modes of the  $0^+$  excited states in even krypton isotopes we report in this work on the results obtained for the  $0_2^+$  state in  $^{80}\text{Kr}$ .

Moreover, an investigation of the excitation pattern and decay properties of low-lying positive-parity levels in  $^{78,80,82}\text{Kr}$  has been performed in the framework of the IBM-2 model, giving a consistent description of the  $0_2^+$  levels within the model space used.

### II. EXPERIMENTAL RESULTS

#### A. Conversion electron measurements

Low-lying levels in  $^{80}\text{Kr}$  were populated via the  $\beta^+$  decay of a source of  $^{80}\text{Rb}$  ( $T_{1/2} = 34$  s). The  $^{80}\text{Rb}$  activity was produced by bombarding a  $34\text{-g/cm}^2$  Nb-foil target with a  $2\text{-}\mu\text{A}$ , 600-MeV proton beam from the CERN Synchrocyclotron. The rubidium atoms were ionized in a W-hot surface ionization source, separated in the ISOLDE on-line mass separator and collected on an aluminum foil. The decay scheme of  $^{80}\text{Rb}$  to levels of  $^{80}\text{Kr}$  [10] is shown in Fig. 1.

Internal conversion electrons were detected by means of a magnetic transport system, described in detail in Ref. [11], which was modified to match the beam characteristics of the ISOLDE separator. The system, coupled to a  $5 \text{ cm}^2 \times 5 \text{ mm}$  Si(Li) detector cooled to liquid-nitrogen temperature, has a momentum acceptance  $\Delta p/p = 18\%$  and an overall full energy peak efficiency of 1%. The energy resolution of the detector is  $\sim 2.6 \text{ keV}$  for 1-MeV electrons. The calibration of the relative efficiency of the spectrometer as a function of the electron energy was performed by means of  $^{207}\text{Bi}$  and  $^{152}\text{Eu}$  sources placed at the target position.

Gamma rays were detected by a HPGe detector (having a resolution of 2.2 keV at 1.33-MeV energy) placed 80 cm away from the target.

The gamma and electron spectra were simultaneously recorded by means of a multiplexed acquisition system. The signal from a high stability pulser at 1-Hz frequency was fed into each acquisition channel to correct for dead-time effects. To reduce the dead time on the electron channel to 15%, we were forced to limit the beam current to  $\approx 2 \times 10^7$  atoms/s because of the high flux of gamma rays on the Si(Li) detector due to annihilation and bremsstrahlung of  $\beta^+$  particles from  $^{80}\text{Rb}$  decay.

The basic quantity to be determined is the ratio  $q^2$

$$q^2 = \frac{I_K(0_2^+ \rightarrow 0_1^+)}{I_K(0_2^+ \rightarrow 2_1^+)} \quad (1)$$

of the  $K$ -conversion electron intensities  $I_K$  for the  $0_2^+ \rightarrow 0_1^+$ , 1320-keV and the  $0_2^+ \rightarrow 2_1^+$ , 704-keV transitions.

Energy spectra of the conversion electrons were recorded for two different magnetic-field settings corresponding to the maximum transmission for the  $K$ -conversion electron line of the two transitions [see Figs. 2(a) and (b)].

To evaluate the integrals of the  $K$ -conversion electron lines, which have an asymmetric shape, the experimental histograms were fitted by a function resulting from the convolution with a Gaussian of a delta function plus an exponential “tail” on the low-energy side. The background was fitted by a second-order polynomial so that altogether an eight parameter fit was performed for each

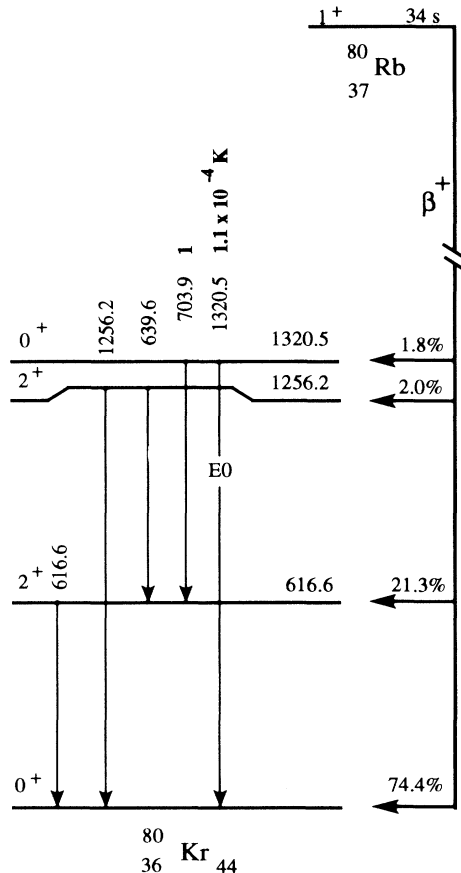


FIG. 1. The decay scheme of  $^{80}\text{Rb}$  (Ref. [10]). The line from the  $0_2^+$  state to the ground state represents the  $E0$  transition studied in this work. The branching for the  $E0$  transition refers to  $K$ -conversion electrons.

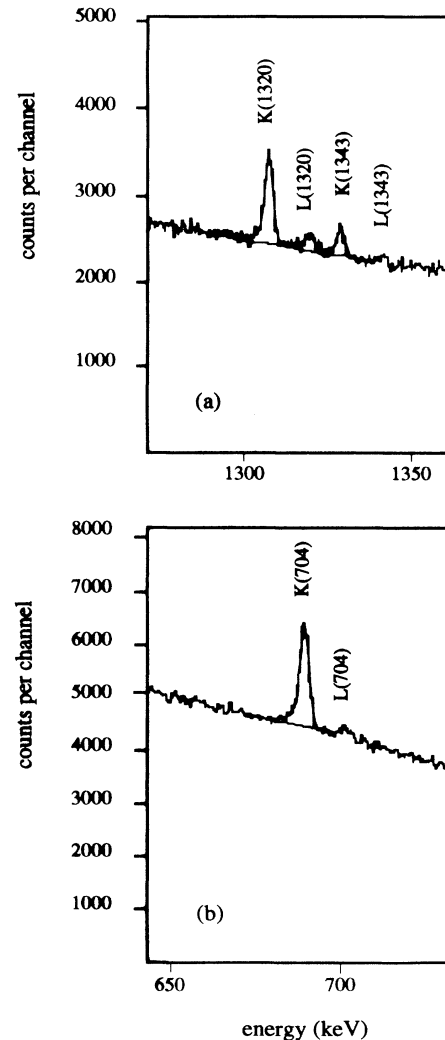


FIG. 2. Relevant sections of the electron energy spectra: (a)  $K$ - and  $L$ -conversion lines of the 1320-keV,  $0_2^+ \rightarrow 0_1^+$  transition and of the 1343-keV transition assigned to  $^{80}\text{Kr}$  (see text). (b)  $K$ - and  $L$ -conversion lines of the 704-keV,  $0_2^+ \rightarrow 2_1^+$  transition.

line. The area of the peaks in the gamma spectra was instead evaluated by fitting a Gaussian curve plus a linear background. Since the electron spectra were recorded at different times, the area of each  $K$ -conversion line was normalized to the intensity of the simultaneously recorded  $2_1^+ \rightarrow 0_1^+$ , 617-keV gamma transition. A 3% correction was applied to take into account the difference in the relative electron efficiency. In this way we obtained for the ratio  $q^2$  the value

$$q^2 = 0.103 \pm 0.011.$$

The ratio  $X = B(E0; 0_2^+ \rightarrow 0_1^+) / B(E2; 0_2^+ \rightarrow 2_1^+)$  of the  $E0$  to  $E2$  reduced transition probability is related to  $q^2$  by the expression [12]

$$X = 2.56 \times 10^9 A^{4/3} E_\gamma^5 (\text{MeV}) \frac{\alpha_K(E2)}{\Omega_K (\text{s}^{-1})} q^2. \quad (2)$$

Here  $\Omega_K$  is the "electronic" factor for the  $K$  conversion of the  $E0$  transition and  $\alpha_K(E2)$  is the  $K$ -conversion coefficient for the  $0_2^+ \rightarrow 2_1^+$  transition. By using the tabulated values of  $\Omega_K$  [13] and  $\alpha_K(E2)$  [14] and the experimental value of  $q^2$ , we derived the value

$$X = 0.022 \pm 0.002.$$

We also tried to identify a possible  $0_3^+$  level which, on the basis of the close similarity between the excitation pattern of  $^{80}\text{Kr}$  and its isotone  $^{78}\text{Se}$  [15], is expected to lie around 2 MeV. From the absence of any conversion line in the energy range 1900–2100 keV, we deduced an upper limit of 0.05 (95% C.L.) for the intensity ratio  $I_K(0_3^+ \rightarrow 0_1^+) / I_K(0_2^+ \rightarrow 0_1^+)$ .

An attempt was also performed to detect an  $E0$  component in the  $2_2^+ \rightarrow 2_1^+$ , 640-keV transition in  $^{80}\text{Kr}$  according to the procedure described in detail in the recent work by Giannatiempo *et al.* [16] on cadmium isotopes. To this end the  $K$ -conversion coefficient  $\alpha_K(640)$  was measured by means of the NPG (normalized peak to gamma) method [17] using the  $2_1^+ \rightarrow 0_1^+$ , 617-keV transition as a reference line. From the value

$$\alpha_K(640) = (1.31 \pm 0.07) \times 10^{-3}$$

and from the value of the mixing ratio  $\delta(E2/M1)$  given in Ref. [10], we deduced an upper limit (95% C.L.) of 0.07 for the intensity ratio of the  $E0$  component to the  $E2$  component of the  $2_2^+ \rightarrow 2_1^+$   $K$ -conversion transition. This translates into the upper limit

$$X = B(E0; 2_2^+ \rightarrow 2_1^+) / B(E2; 2_2^+ \rightarrow 2_1^+) \leq 0.028 \quad (95\% \text{ C.L.}).$$

Figure 2(a) shows a peak at an electron energy of  $1328.76 \pm 0.20$  keV while in the corresponding gamma spectrum there is a strong line at an energy of  $1343.09 \pm 0.06$  keV which has not previously been reported in the literature. The energy difference of  $14.33 \pm 0.21$  keV closely matches the binding energy of a  $K$  electron in krypton ( $\epsilon_K = 14.326$  keV) and is incompatible with the  $\epsilon_K$  of any other element. Furthermore, not even the most intense lines from other krypton isotopes are present in the gamma spectrum. We thus assign the 1343-keV line as corresponding to a transition in  $^{80}\text{Kr}$ . The measured value of its  $K$ -conversion coefficient [ $\alpha_K(1343) = (0.209 \pm 0.025) \times 10^{-3}$ ] implies an  $E2$  or  $M1$  multipolarity.

### B. Lifetime of the $0_2^+$ state

To measure the lifetime of the  $0_2^+$  state at 1320 keV we used the Doppler shift attenuation method (DSA) in gases [18,19]. The level was populated via the  $(p, p')$  reaction on a gas target. A sample of krypton gas (42% enriched in  $^{80}\text{Kr}$ ) was bombarded by the proton beam from the CN van de Graaff accelerator of the Laboratori Nazionali di Legnaro (Padua). The gas was contained in a small chamber (described in detail in Ref. [20]) which had a  $3\text{-mg/cm}^2$  nickel entrance window. The gas pressure was measured to an accuracy of  $\pm 5\%$  by a standard pressure gauge. The proton beam energy was fixed at 6.5 MeV in order to avoid the opening of the  $(p, n)$  reaction channel on  $^{80}\text{Kr}$ .

Gamma rays were recorded by means of a HPGe detector having a resolution of 2.5 keV at 1.33 MeV. The detector was positioned at  $0^\circ$  to the beam direction, at a

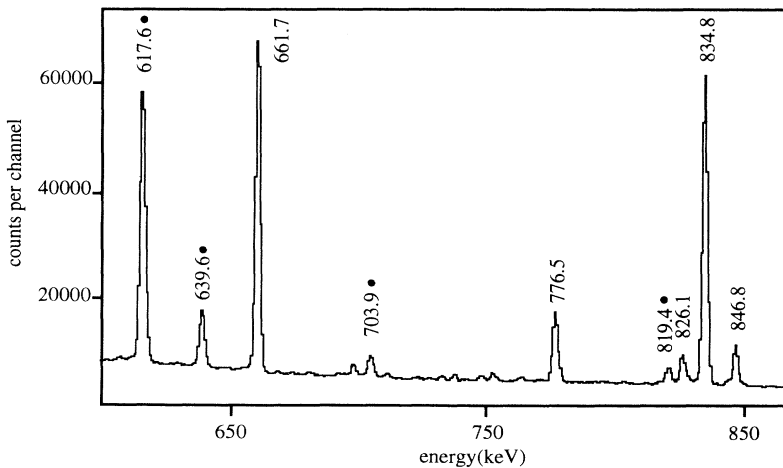


FIG. 3. Part of the gamma energy spectrum produced by the 6.5 MeV  $(p, p')$  reaction on the enriched krypton gas at a pressure of  $9 \times 10^5$  Pa. Peaks corresponding to  $\gamma$  transitions in  $^{80}\text{Kr}$  are marked by a black dot.

distance of 125 mm from the center of the gas chamber, and was shielded by a 75-mm-thick paraffin layer to reduce the flux of fast neutrons produced via the  $(p, n)$  reaction on the nickel window and on  $^{82,84}\text{Kr}$ . The beam current was varied in the 5–15 nA range in keeping with the target thickness (i.e., the gas pressure) to maintain an approximately constant counting rate. Since the measurement was based on the accurate determination (as a function of the gas target pressure) of the centroid of the 704-keV gamma ray deexciting the  $0_2^+$  state, sources of  $^{137}\text{Cs}$  and  $^{55}\text{Mn}$  were utilized to provide an in-beam calibration of the energy scale. An example of the gamma energy spectrum recorded for a pressure of  $9 \times 10^5$  Pa is shown in Fig. 3. Altogether gamma spectra were recorded for  $N=9$  different pressures, ranging from  $2 \times 10^5$  to  $50 \times 10^5$  Pa.

The essence of the DSA method in gases is to compare (for each gas pressure  $P_i$ ) the measured centroid  $E_i^{\text{ex}}$  of the full energy peak for the deexciting gamma ray, with the value  $E_i^{\text{th}}$  calculated, on the basis of a given theory of the energy loss and angular straggling of the recoil nuclei (see below), under the assumption of a given lifetime  $\tau$  of the level of interest.

For the data analysis we adopted a minimum  $\chi^2$  procedure based on the statistics (with an obvious notation):

$$\chi^2 = \sum_i^{1, \dots, N} \frac{(E_i^{\text{th}} - E_i^{\text{ex}})^2}{\sigma_i^2}. \quad (3)$$

$$g_i^{\text{th}} = 1 + \frac{\int_0^D Y(z) dz \int_0^\pi W(\cos\theta_0, z) \beta(\cos\theta_0, z) \cos\theta(\cos\theta_0, z) F(\tau, P_i, \beta) 2\pi \sin\theta_0 d\theta_0}{\int_0^D Y(z) dz \int_0^\pi W(\cos\theta_0, z) 2\pi \sin\theta_0 d\theta_0}. \quad (5)$$

We measured the excitation function  $Y(z)$  for the gamma rays of interest by bombarding the krypton target at a pressure of  $10^5$  Pa and varying the proton beam energy in steps of 100 keV over the range 4.5–6.5 MeV (for the 704-keV line, already at an energy of about 5 MeV, the yield drops to 10% of the maximum value). For the

In this expression  $E_i^{\text{th}}$  is proportional to the unshifted gamma-ray energy  $E_0$  ( $E_i^{\text{th}} = g_i^{\text{th}} E_0$ ) which is considered as a free parameter. We have therefore  $N-2$  degrees of freedom for  $\chi^2$ . For each assumed value of  $\tau$ , we then numerically calculated the  $N$  values of  $g_i$  and deduced the value of  $E_0$  which minimizes  $\chi^2$ . The corresponding value of  $\chi^2(\tau)$  is then derived by inserting in (3) the value of  $E_i^{\text{th}}$ .

As is well known, the attenuation of the maximum Doppler shift of a  $\gamma$  ray of energy  $E_0$  emitted by a nucleus moving with an initial velocity  $\beta$  ( $c=1$ ) at an angle  $\theta$  with respect to the detector axis, is described, for each pressure  $P_i$ , by the attenuation factor

$$F_i = \frac{E_i^{\text{ex}} - E_0}{E_0 \beta \cos\theta}, \quad (4)$$

where we neglect any effect due to the finite solid angle subtended by the detector due to the large detector-source distance in our setup.

In our case, however, we must take into account that the recoil nuclei are produced at different depths  $z$  in the target (hence with different energies of impinging protons), with different yields  $Y(z)$  and c.m. angular distribution  $W(\cos\theta_0, z)$  so that the theoretical value  $g_i^{\text{th}}$  should be calculated as a weighted average over the target thickness  $D$  and over the angular distribution  $W(\cos\theta_0, z)$ . In formula, for a given pressure  $P_i$  and each assumed value of  $\tau$ , we have

function  $W(\cos\theta_0, z)$ , in the absence of any experimental information, we have generally assumed an energy-independent isotropic angular distribution of the recoil nuclei in the center-of-mass system. Some alternative schematic angular distributions have also been considered (see below). In all the calculations the angular

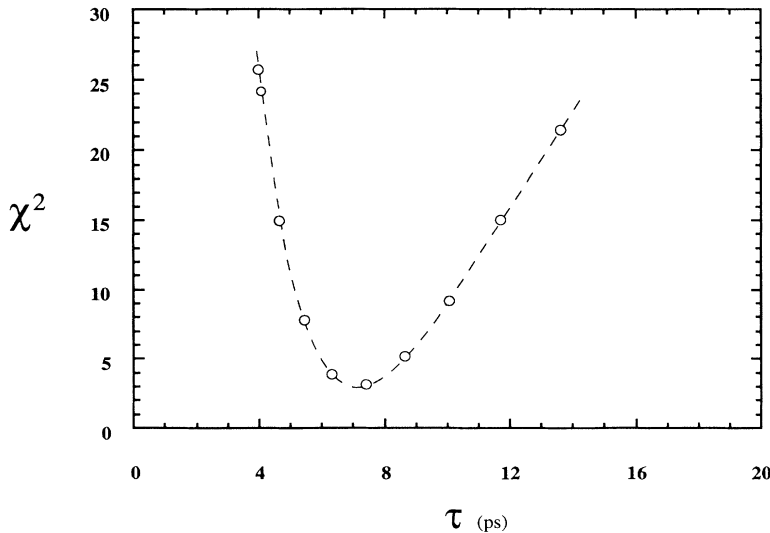


FIG. 4. The value of  $\chi^2$  minimized with respect to variation of the unshifted  $\gamma$ -ray energy  $E_0$  is reported as a function of the assumed value of the lifetime  $\tau$  of the 1320-keV level.

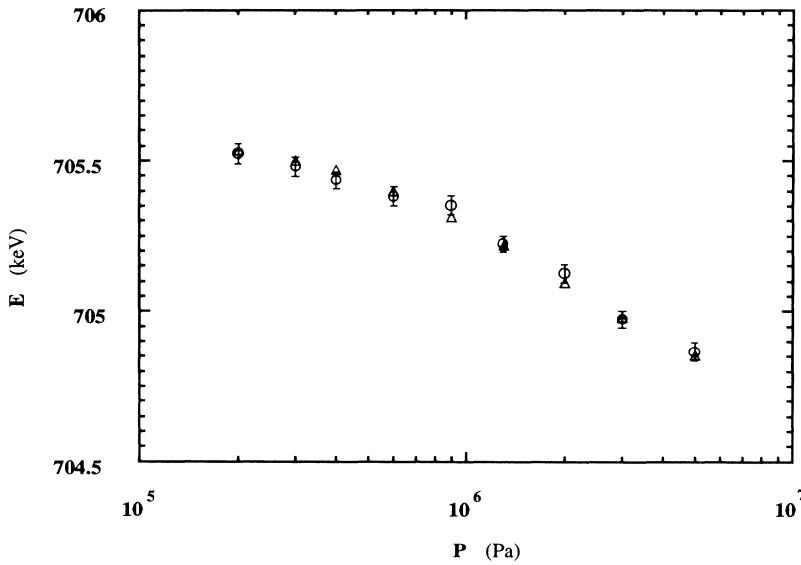


FIG. 5. The measured energy of the gamma ray for the  $0_2^+ \rightarrow 2_1^+$  transition is reported as a function of the gas pressure. The triangles are the calculated values of the energy obtained via a minimum  $\chi^2$  procedure.

straggling of krypton nuclei during the slowing down process was treated in the Blaugrund approximation [21].

For what concerns the energy loss of ions in gases, no study as detailed as for the corresponding case of recoiling nuclei in solids [22] has been reported. In such a situation it seemed to us reasonable to adopt as a starting point the Lindhard-Scharff-Schiøtt (LSS) theory [23], and to introduce adjustment factors  $f_e$  and  $f_n$  for the electronic and nuclear part of the energy loss, respectively (as in Ref. [24]). The parameter  $f_e$  has very little influence on the results of data analysis since the energy loss at low recoil velocity (as is the case of our experiment,  $\beta \approx 0.001$ ) is dominated by the nuclear part. For  $f_e$  we then adopted the value  $f_e = 0.9$  reported in Ref. [24] for nuclei of this mass region. The parameter  $f_n$  was varied so as to reproduce the experimental value of the lifetime of the  $2_2^+$  level at 1256 keV ( $\tau = 11 \pm 2$  ps, Ref. [25]). Indeed, this lifetime has been measured, following heavy-ion reactions, by the recoil distance method which is essentially free from uncertainties on the energy loss. We found that the experimental value of the lifetime is closely reproduced for  $f_n = 0.7$ . It might be interesting to remark that the lifetime of all the levels below 2-MeV excitation energy in  $^{80}\text{Kr}$  has been measured [10] by the recoil distance method with the only exception the  $0_2^+$  level, which is hardly populated in heavy-ion reactions. We then applied the minimum  $\chi^2$  procedure to determine the lifetime of the 1320-keV level and found a minimum of  $\chi^2$  for  $\tau$  around 7 ps for which we evaluated, by the method of Cline and Lesser [26], a statistical uncertainty of  $\pm 1$  ps (68% C.L.).

In Fig. 4 the  $\chi^2$  value is reported as a function of the assumed lifetime (in each case for the best-fitted unperturbed gamma-ray energy  $E_0$ ) while the best fit to the experimental data is shown in Fig. 5. It is worth mentioning that we repeated the whole procedure by assuming for the recoiling krypton nuclei energy-independent c.m. angular distributions of the type  $W(\cos\theta_0) \propto [1 + a \cos\theta_0]$  and  $[1 + a \cos^2\theta_0]$  for different values of the parameter  $a$  in the range  $-0.2$  to  $+0.2$  and failed to improve the nor-

malized minimum value of  $\chi^2$ . From these calculations we estimate that the overall uncertainty on the lifetime value due to the ignorance of the angular distribution could be as large as  $\pm 2$  ps.

By combining quadratically the different error sources we arrive at an estimate of  $\pm 3$  ps for the total uncertainty, so that our final result for the lifetime of the  $0_2^+$  level at 1320 keV reads

$$\tau(1320) = 7 \pm 3 \text{ ps} .$$

From this value we deduce  $B(E2; 0_2^+ \rightarrow 2_1^+) = 670 \pm 280 e^2 \text{ fm}^4$ .

The electric monopole strength  $\rho^2$  is connected to the quantities  $X$  and  $B(E2)$  via the relation

$$\rho^2(E0) = \frac{XB(E2)}{e^2 R^4} , \quad (6)$$

where  $R$  is the nuclear radius given by the expression  $R = 1.2 A^{1/3}$  fm. From the results given above we find

$$\rho^2(E0; 0_2^+ \rightarrow 0_1^+) = 0.021 \pm 0.009 .$$

For the  $2_2^+ \rightarrow 2_1^+$  transition we used the value of  $B(E2; 2_2^+ \rightarrow 2_1^+)$  given in Ref. [25] and our upper limit for  $X$  to obtain

$$\rho^2(E0; 2_2^+ \rightarrow 2_1^+) < 0.05 \text{ (95\% C.L.)} .$$

### III. DISCUSSION AND CONCLUSIONS

As mentioned above, the question of whether the  $0_2^+$  states in krypton isotopes are to be considered as “in-

TABLE I. Adopted values for the Hamiltonian parameters used for IBA-2 calculations. All parameters are given in MeV, except for  $\chi_v$  and  $\chi_\pi$  (dimensionless).

	$\kappa$	$\epsilon$	$\chi_v$	$\chi_\pi$	$w_{vv} = w_{v\pi}$	$\xi_2$	$\xi_3$
$^{78}\text{Kr}$	-0.095	0.770	-1.1	-0.1	0.018	0.060	-0.21
$^{80}\text{Kr}$	-0.095	0.865	-1.1	-0.1	0.018	0.075	-0.21
$^{82}\text{Kr}$	-0.095	0.955	-1.1	-0.1	0.018	0.090	-0.21

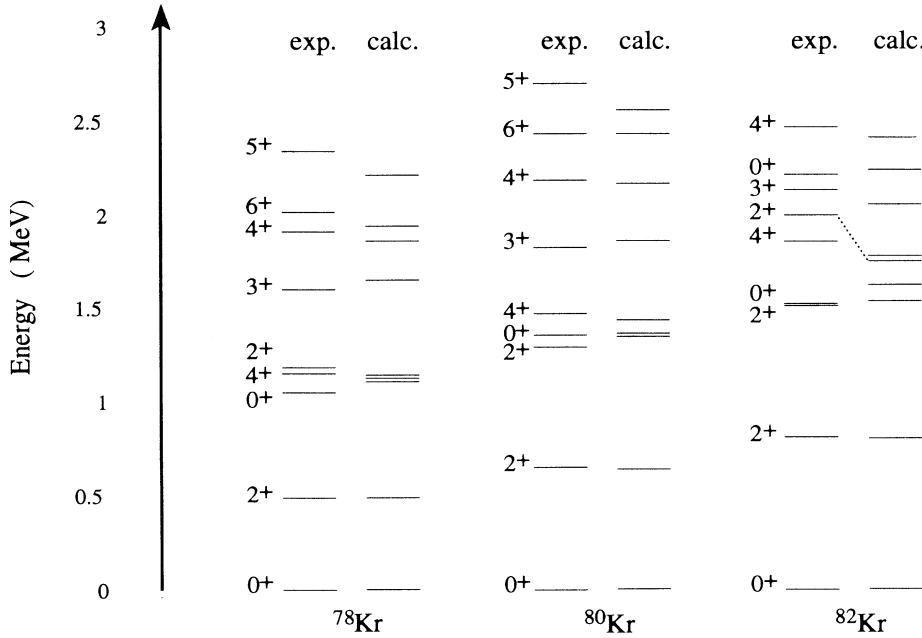


FIG. 6. Calculated and experimental excitation energies of low-lying positive-parity states in  $^{78,80,82}\text{Kr}$ . Only experimental levels of definite spin and parity assignment are displayed. Accordingly a few low-lying levels predicted by the theory are omitted. The spin sequence reported on the left-hand side for each nucleus refers also to the levels predicted by the theory, except for the  $2_3^+$  state in  $^{82}\text{Kr}$ , as indicated.

truder” or as belonging to the IBM model space has not yet received a satisfactory answer. In an attempt to favor a choice between the two interpretations, we have calculated, in the framework of the IBM-2 model, excitation energies,  $E2$  and  $E0$  transition strengths, and  $E2/M1$  mixing ratios for low-lying positive-parity levels in  $^{78,80,82}\text{Kr}$ .

The calculations were performed by means of the computer code NPBOS [27] adopting for the Hamiltonian the parameter values reported in Table I (in the notation of Ref. [27]). This set of parameters was obtained through a systematic search having as basic points the determination of the  $d$ -boson energy  $\epsilon$  and of the parameters  $\kappa$ ,  $\chi_\pi$ , and  $\chi_\nu$  which fix the strength of the quadrupole proton-

neutron boson interaction. The dipole interaction terms  $\hat{L}_\nu \cdot \hat{L}_\nu$  and  $\hat{L}_\nu \cdot \hat{L}_\pi$  were also explicitly considered in the Hamiltonian and their strength, given by the parameters  $w_{\nu\nu}$  and  $w_{\nu\pi}$ , was kept constant for the three nuclei. For the parameter  $\kappa$  we used as a starting point a value such that the corresponding value in the IBM-1 space (obtained according to the projection procedure given in Ref. [28]) would be close to that used by Erokhina *et al.* [8] in their IBM-1 calculations. The value of  $\epsilon$  is essentially fixed by the energies of the  $2_1^+$  states. For the determination of  $\chi_\pi$  and  $\chi_\nu$  (which appear also in the standard IBM-2 expression for the quadrupole operator) we followed the procedure outlined in Ref. [29], which, besides excitation energies, also exploits those  $B(E2)$

TABLE II. Experimental and theoretical values for  $B(E2)$  transition strengths (given in  $e^2 b^2$ ) in  $^{78,80,82}\text{Kr}$ . The values  $e_\pi = 0.075 e b$ ,  $e_\nu = 0.090 e b$  for boson effective charges have been used.

$J_i^+ \rightarrow J_f^+$	$^{78}\text{Kr}$		$^{80}\text{Kr}$		$^{82}\text{Kr}$	
	Expt. <sup>a</sup>	Theor.	Expt. <sup>b</sup>	Theor.	Expt. <sup>d</sup>	Theor.
$0_2^+ \rightarrow 2_1^+$			0.07(3) <sup>c</sup>	0.07	0.030(10)	0.055
$0_3^+ \rightarrow 2_1^+$					0.005(4)	0.0001
$2_1^+ \rightarrow 0_1^+$	0.120(8)	0.097	0.076(6)	0.071	0.044(2)	0.051
$2_2^+ \rightarrow 0_1^+$	0.0030(4)	0.0020	0.0006(1)	0.0010	0.0002(1)	0.0006
$2_2^+ \rightarrow 2_1^+$	0.012(4)	0.086	0.05(1)	0.07	0.016(8)	0.030
$2_3^+ \rightarrow 0_1^+$					0.0006(4)	$4 \times 10^{-5}$
$2_3^+ \rightarrow 2_1^+$					0.014(8)	0.036
$3_1^+ \rightarrow 2_1^+$			0.0012(2)	0.0009		
$3_1^+ \rightarrow 2_2^+$			0.072(10)	0.048		
$4_1^+ \rightarrow 2_1^+$	0.174(14)	0.152	0.064(6)	0.111	0.065(24)	0.078
$4_2^+ \rightarrow 2_1^+$			0.0007(4)	0.0014	0.024(6)	0.001
$4_2^+ \rightarrow 2_2^+$	0.115(16)	0.063	0.10(5)	0.04	0.018(5)	0.028
$4_2^+ \rightarrow 4_1^+$	0.05(1)	0.04	0.07(4)	0.02	0.08(2)	0.009
$6_1^+ \rightarrow 4_1^+$	0.20(3)	0.17	0.13(3)	0.12		

<sup>a</sup>Reference [15].

<sup>b</sup>Reference [10].

<sup>c</sup>Present work.

<sup>d</sup>Reference [30].

TABLE III. Experimental and theoretical values of the mixing ratios  $\delta$  in  $^{78,80,82}\text{Kr}$ .

$J_i^+ \rightarrow J_f^+$	$^{78}\text{Kr}$		$^{80}\text{Kr}$		$^{82}\text{Kr}$	
	Expt. <sup>a</sup>	Theor.	Expt. <sup>b</sup>	Theor.	Expt. <sup>c</sup>	Theor.
$2_2^+ \rightarrow 2_1^+$	0.5(1)	3.9	6(1)	1.9	$2.7^{+1.0}_{-0.5}$	0.7
$3_1^+ \rightarrow 2_1^+$			1.3(3)	0.7	$5.7^{+5.2}_{-1.7}$	0.9
$3_1^+ \rightarrow 2_2^+$			3.0(4)	0.8	3.1(6)	1.5
$4_2^+ \rightarrow 4_1^+$			2.0(8)	0.5	$0.1^{+1.9}_{-0.4}$	0.2
$5_1^+ \rightarrow 4_1^+$	2(1)	0.7	0.8(3)	0.7		

<sup>a</sup>Reference [32].<sup>b</sup>Reference [25].<sup>c</sup>Reference [33].

transition rates which are particularly sensitive to these parameters and the  $E2/M1$  mixing ratios. In particular, the sign of  $\delta$  provides a useful constraint on the sign of  $\chi_\pi$  and  $\chi_\nu$ . Indeed it is found that a simultaneous sign reversal of  $\chi_\pi$  and  $\chi_\nu$  [which does not affect the calculated values of excitation energies and  $B(E2)$  rates] changes accordingly the sign of  $\delta$ .

In Fig. 6 the experimental [10,15,30] and calculated excitation patterns of the low-energy region in  $^{78,80,82}\text{Kr}$  are compared. The overall agreement is quite reasonable and the  $0^+$  states do not show any particular deviation.

For the  $E2$  transitions, the effective boson charges  $e_\pi$  and  $e_\nu$  were determined by a fit to those  $B(E2)$  transition rates which are only slightly affected by the values of  $\chi_\pi$  and  $\chi_\nu$ . The calculated and experimental values of  $B(E2)$  transition rates are given in Table II. It is seen that a good general agreement is obtained, equivalent to that found by several previous authors [4–7]. In particular, the  $B(E2)$  transition strengths from the  $0^+$  states are also quite reasonably reproduced. We remark that for the quadrupole moments of the  $2_1^+$  states in  $^{78,80,82}\text{Kr}$  (which unfortunately have not been measured) we calculated the values  $-0.46$ ,  $-0.33$ , and  $-0.24$  e b, respectively, which are close to those reported in the literature [31] for the  $2_1^+$  state in the isotones  $^{76,78,80}\text{Se}$  and  $^{74,76}\text{Ge}$ .

For the calculations of the mixing ratios  $\delta$ , we used, in the standard IBM-2 expression of the  $M1$  operator, the effective  $g$  factors  $g_\pi = 0.7\mu_N$  and  $g_\nu = 0.4\mu_N$ . The available experimental data [25,32,33] on the mixing ratio  $\delta$  together with the corresponding calculated values are shown in Table III; it is seen that the signs are correctly reproduced. We remind the reader that the sign of the  $M1$  matrix element only depends on the difference  $g_\pi - g_\nu$  (always assumed positive in the literature) and

not on their particular values. With the adopted values of  $g_\pi$  and  $g_\nu$  we can reproduce the value of the magnetic dipole moment of the  $2_1^+$  state in  $^{78}\text{Kr}$  [31], which is the only one known in these nuclei.

Finally, we calculated the electric monopole transition rates. In the IBM-2 model the  $E0$  transition operator has the following expression:

$$\hat{T}(E0) = \beta_{0\nu} \hat{n}_{d_\nu} + \beta_{0\pi} \hat{n}_{d_\pi}, \quad (7)$$

where  $\hat{n}_{d_{\nu(\pi)}}$  is the number of  $d$ -neutron (proton) bosons and  $\beta_{0\nu(\pi)}$  is the so-called neutron (proton) monopole boson effective charge. The monopole strength  $\rho^2$  is related to  $\hat{T}(E0)$  by the expression

$$\rho^2(E0; J_i^+ \rightarrow J_f^+) = \frac{Z^2}{e^2 R^4 (2J_i + 1)} [\beta_{0\nu} \langle J_f | \hat{n}_{d_\nu} | J_i \rangle + \beta_{0\pi} \langle J_f | \hat{n}_{d_\pi} | J_i \rangle]^2. \quad (8)$$

Due to the paucity of experimental data on  $\rho^2$  for krypton isotopes, we choose for the parameters  $\beta_{0\nu}$  and  $\beta_{0\pi}$  the values derived in Ref. [16] from a detailed analysis of  $E0$  transitions in  $^{110,112,1124}\text{Cd}$  nuclei, namely,  $\beta_{0\nu} = 0.25$  e fm<sup>2</sup> and  $\beta_{0\pi} = 0.10$  e fm<sup>2</sup>. The strength of the  $E0$  decay mode is quite satisfactorily reproduced, as seen in Table IV, where the calculated and experimental value of  $\rho^2$  are compared.

To summarize, the present analysis shows that an interpretation of the  $0_2^+$  states in  $^{78,80,82}\text{Kr}$  nuclei in terms of the standard IBM-2 model is still possible, thus making it unnecessary to invoke the admixture of more complicated configurations.

#### ACKNOWLEDGMENTS

We would like to thank I. Motti from Laboratori Nazionali di Legnaro for his efficient cooperation. The authors are indebted to Dr. P. Del Carmine, A. Pecchioli, and M. Ottanelli for their important technical support. Our thanks are also due to Professor T. Fazzini for his patient and precious collaboration, Professor M. Pignanelli, and Dr. G. Maino for many helpful discussions.

TABLE IV. The experimental values of  $\rho^2(E0)$  in  $^{80,82}\text{Kr}$  are compared to the theoretical ones evaluated using for the  $E0$  operator the parameters values  $\beta_{0\nu} = 0.25$  e fm<sup>2</sup>,  $\beta_{0\pi} = 0.1$  e fm<sup>2</sup>.

$\rho^2(J_i^+ \rightarrow J_f^+)$	$^{80}\text{Kr}$		$^{82}\text{Kr}$	
	Pres. work	Theor.	Refs. [6,9]	Theor.
$0_2^+ \rightarrow 0_1^+$	0.021(9)	0.032	0.008(3)	0.014
$2_2^+ \rightarrow 2_1^+$	$\leq 0.05$	0.002		
$0_3^+ \rightarrow 0_1^+$			0.007(6)	0.001

- [1] J. H. Hamilton, Nucl. Phys. **A520**, 377 C (1990).
- [2] U. Kaup and A. Gelberg, Z. Phys. A **293**, 311 (1979).
- [3] B. Wörmann *et al.*, Nucl. Phys. **A431**, 170 (1984).
- [4] H. P. Hellmeister *et al.*, Phys. Lett. **85B**, 34 (1979).
- [5] H. P. Hellmeister *et al.*, Nucl. Phys. **A332**, 241 (1979).
- [6] S. Brüssermann *et al.*, Phys. Rev. C **32**, 1521 (1985).
- [7] A. F. Barfield and K. P. Lieb, Phys. Rev. C **41**, 1762, (1990).
- [8] K. I. Erokhina *et al.*, Izv. Akad. Nauk. SSSR, Ser. Fiz **48**, 328 (1984).
- [9] A. Zemel, T. Hageman, J. J. Hamill, and J. van Klinken, Phys. Rev. C **31**, 1483 (1985).
- [10] T. B. Singh and D. A. Viggars, Nucl. Data Sheets **36**, 203 (1982).
- [11] T. Fazzini, A. Giannatiempo, and A. Perego, Nucl. Instrum. Methods **211**, 125 (1983).
- [12] A. V. Aldushenkov and N. A. Voinova, Nucl. Data Tables **11**, 299 (1973).
- [13] A. Passoja and T. Salonen, University of Jyväskylä Research Report No. 2, 1986.
- [14] F. Rösel, H. M. Fries, K. Alder, and H. C. Pauli, At. Data Nucl. Data Tables **21**, 91 (1978).
- [15] S. Rab, Nucl. Data Sheets **63**, 1 (1991).
- [16] A. Giannatiempo, A. Nannini, A. Perego, and P. Sona, Phys. Rev. C **44**, 1844 (1991).
- [17] H. C. Pauli, K. Alder, and R. M. Steffen, in *The Electromagnetic Interaction in Nuclear Spectroscopy*, edited by W. D. Hamilton (North-Holland, Amsterdam, 1975), p. 451.
- [18] M. Bini, P. G. Bizzeti, A. M. Bizzeti Sona, and R. A. Ricci, Phys. Rev. C **6**, 784 (1972).
- [19] M. Bini, P. G. Bizzeti, and R. Fabene, J. Phys. G **12**, 223 (1986).
- [20] M. Bini, G. Poggi, and N. Taccetti, Nucl. Instrum. Methods **212**, 235 (1983).
- [21] A. E. Blaugrund, Nucl. Phys. **88**, 501 (1966).
- [22] J. F. Ziegeler, J. P. Biersack, and U. Littmark, *The Stopping and Range of Ions in Solids* (Pergamon, New York, 1985).
- [23] J. Lindhard, M. Scharff, and H. E. Schiøtt, Mat. Fys. Medd. Dan. Vid. Selsk. **33**, No. 14 (1963).
- [24] A. A. Alexandrov, M. P. Kudoyarov, I. Kh. Lemberg, and A. A. Pasternak, Nucl. Phys. **A321**, 189 (1979).
- [25] L. Funke *et al.*, Nucl. Phys. **A355**, 228 (1981).
- [26] D. Cline and P. S. Lesser, Nucl. Instrum. Methods **82**, 291 (1970).
- [27] T. Otsuka and N. Yoshida, Program NPBOS, Japan Atomic Energy Research Institute Report JAERI-M85-094, 1985.
- [28] A. Novoselsky and I. Talmi, Phys. Lett. **160B**, 13 (1985).
- [29] A. Giannatiempo, A. Nannini, A. Perego, P. Sona, and G. Maino, Phys. Rev. C **44**, 1508 (1991).
- [30] H. W. Müller, Nucl. Data Sheets **50**, 1 (1987).
- [31] P. Raghavan, Atomic Data Nucl. Data Tables **42**, 189 (1989).
- [32] R. L. Robinson *et al.*, Phys. Rev. C **21**, 603 (1980).
- [33] R. A. Meyer *et al.*, Phys. Rev. C **27**, 2217 (1983).